

2
3 **Differential mobilization of terrestrial carbon pools in Eurasian Arctic river basins**

4 Shorter title: Terrestrial carbon mobilization in the Arctic

5 Xiaojuan Feng^{a,b,1}, Jorien E. Vonk^{a,c}, Bart E. van Dongen^d, Örjan Gustafsson^e, Igor P. Semiletov^{f,g},
6 Oleg V. Dudarev^g, Zhiheng Wang^h, Daniel B. Montluçon^{a,b}, Lukas Wackerⁱ and Timothy I.
7 Eglinton^{a,b}

8
9 ^aGeological Institute, ETH Zürich, 8092 Zürich, Switzerland

10 ^bDepartment of Marine Chemistry and Geochemistry, Woods Hole Oceanographic Institution,
11 Woods Hole, MA 02543, USA

12 ^cDepartment of Earth Sciences, Utrecht University, 3584 CD, Utrecht, the Netherlands

13 ^dSchool of Earth, Atmospheric and Environmental Sciences (SEAES) and the Williamson Research
14 Centre for Molecular Environmental Science, University of Manchester, Manchester, M13 9PL, UK

15 ^eDepartment of Applied Environmental Science (ITM) and the Bolin Centre for Climate Research,
16 Stockholm University, 10691, Stockholm, Sweden

17 ^fInternational Arctic Research Center (IARC), University of Alaska Fairbanks, Fairbanks, USA

18 ^gPacific Oceanological Inst., Russian Academy of Sciences, Far Eastern Branch (FEBRAS),
19 Vladivostok, Russia

20 ^hCenter for Macroecology, Evolution and Climate, Department of Biology, University of
21 Copenhagen, DK-2100, Copenhagen, Denmark

22 ⁱLaboratory of Ion Beam Physics (LIP), ETH Zürich, 8093 Zürich, Switzerland

¹ To whom correspondence should be addressed. E-mail: xfeng@erdw.ethz.ch; Phone: + 41-44-632 2848; Fax: +41-44-633 1296. Current address: Institute of Botany, Chinese Academy of Sciences, 100093 Beijing, China. Email: xfeng@ibcas.ac.cn.

23 **Abstract**

24 **Mobilization of Arctic permafrost carbon is expected to increase with warming-induced**
25 **thawing. However, this effect is challenging to assess due to the diverse processes controlling**
26 **the release of various organic carbon (OC) pools from heterogeneous Arctic landscapes. Here,**
27 **by radiocarbon dating various terrestrial OC components in fluvially- and coastally-**
28 **integrated estuarine sediments, we present a unique framework for deconvoluting the**
29 **contrasting mobilization mechanisms of surface versus deep (permafrost) carbon pools across**
30 **the climosequence of the Eurasian Arctic. Vascular-plant-derived lignin phenol ¹⁴C contents**
31 **reveal significant inputs of young carbon from surface sources whose delivery is dominantly**
32 **controlled by river runoff. In contrast, plant wax lipids predominantly trace ancient**
33 **(permafrost) OC that is preferentially mobilized from discontinuous permafrost regions**
34 **where hydrological conduits penetrate deeper into soils and thermokarst erosion occurs more**
35 **frequently. As river runoff has significantly increased across the Eurasian Arctic in recent**
36 **decades, we estimate from an isotopic mixing model that, in tandem with an increased**
37 **transfer of young surface carbon, the proportion of mobilized terrestrial OC accounted for by**
38 **ancient carbon has increased by 3-6% between 1985 –2004 findings suggest that, while**
39 **partly masked by surface-carbon export, climate-change-induced mobilization of old**
40 **permafrost carbon is well under way in the Arctic.**

41
42 **Keywords:** fluvial mobilization | compound-specific ¹⁴C | hydrogeographic control

43

44 **Introduction**

45 Arctic permafrost, storing approximately half of the global reservoir of soil OC (1), is
46 suggested to be highly sensitive to warming-induced perturbation and mobilization (2). While
47 increased respiration of permafrost carbon has recently been documented with warming (3) and
48 thawing (4) in Arctic soils, information on the large-scale mobilization of old carbon deposits via
49 fluvial and coastal processes remains sparse (5, 6). As permafrost thaws, the active layer deepens
50 and landscape structures collapse and erode, potentially releasing OC of older ages from deeper
51 horizons into rivers and/or coastal oceans (2, 5, 7). Alteration in permafrost coverage also affects
52 the availability of various hydrological conduits and thus mobilization pathways of OC associated
53 with different permafrost depths and structures (6, 8). As important processes of carbon dispersal in
54 the Arctic, fluvial transport and erosion are hence sensitive to climatic and hydrological changes (8-
55 12). Furthermore, Arctic rivers provide an integrating perspective on carbon release from various
56 OC pools associated with heterogeneous physiogeographic regimes in corresponding drainage
57 basins (13). The central challenge to detecting climate-induced mobilization of permafrost is to
58 distinguish the aged permafrost carbon among the diverse OC components carried in rivers (ranging
59 from modern vegetation debris and plankton to ancient sedimentary rock) (5, 14, 15) and to separate
60 the effect of warming from other hydrogeographic controls on carbon export from different pools.

61 Source-tracing organic molecules offer a unique perspective into the fate of specific carbon
62 pools during fluvial and coastal transport (6, 16-19). As the second most abundant biopolymer and
63 rigidifying tissue in terrestrial vascular plants, lignin represents both an excellent tracer and a
64 quantitatively significant fraction of terrestrial OC (20). The radiocarbon age of lignin-derived
65 phenols in sediments potentially provides an additional dimension of information on the source
66 (recent surface OC versus old permafrost OC) and mobilization pathways of higher plant-derived
67 carbon in the Arctic. Furthermore, Arctic soils contain significant carbon inputs from moss-
68 dominated peat (21, 22), which represents 17% of permafrost carbon in the Northern Hemisphere
69 (1). While this carbon pool does not contain lignin, it can be traced by hydroxy phenols (including
70 *p*-hydroxybenzaldehyde, *p*-hydroxyacetophenone and *p*-hydroxybenzoic acid) that occur in higher
71 abundances in mosses and peat than in vascular plants (23-25). Here, we examine the radiocarbon
72 signature of lignin-derived and hydroxy phenols in estuarine surface sediments across the Eurasian

73 Arctic to compare the fate of various terrestrial OC pools transported over continental drainage
74 basin scales and to exploit their ^{14}C signals as tracers for permafrost-carbon mobilization.

75 Using estuarine sediments as natural integrators of coastal and drainage basin processes, this
76 study includes the estuaries of five Great Russian Arctic Rivers (GRARs: Ob, Yenisey, Lena,
77 Indigirka and Kolyma), extended westward by the Kalix River draining Scandinavia north of the
78 Arctic Circle (Fig. 1). The transect covers a continent-scale climate gradient from west to east (Fig.
79 2a and Table S1). The three eastern GRARs (Lena, Indigirka and Kolyma) are predominantly
80 located in the continuous permafrost region with a drier and colder climate (26). This contrasts with
81 the two western GRARs (Ob and Yenisey) and the Kalix River, which drain a wetter region rich in
82 peatland and wetlands underlain by discontinuous permafrost (27, 28). These contrasting drainage
83 basin characteristics allow us to investigate the hydroclimatic processes controlling the release and
84 transport of Arctic carbon pools.

85

86 **Results and Discussion**

87 **Contrasting ^{14}C characteristics of terrestrial OC components.** We employed a recently modified
88 method (29) to isolate lignin and hydroxy phenols from sedimentary matrices for compound-
89 specific radiocarbon analysis. The radiocarbon content of OC components from estuarine surface
90 sediments affords an average age of terrestrial OC released from the adjacent fluvial drainage basin
91 and via coastal erosion processes. Individual lignin phenols exhibited relatively uniform $\Delta^{14}\text{C}$
92 values (-402 to -367 ‰) in the Indigirka and Kolyma sediments whereas much higher isotopic
93 variability was observed in sediments from the Kalix and Ob (Fig. S1a), implying greater
94 heterogeneity in lignin sources and/or more complex mobilization pathways in the western Eurasian
95 Arctic watersheds. Nevertheless, there was no significant age offset between vanillyl and syringyl
96 phenols in the same estuarine sediments (t test; $P > 0.05$; Fig. S1b). Concentration-weighted
97 average $\Delta^{14}\text{C}$ values of lignin phenols ranged from -385 to $+33$ ‰ across the Eurasian Arctic
98 transect, corresponding to conventional radiocarbon ages of 3,800 yr to modern (Fig. 2b). It is
99 notable that lignin phenols largely follow the trend of bulk OC radiocarbon ages (ranging from 570
100 to 7,500 yr; Fig. 2b), reflecting the role of lignin as a tracer of a major fraction of terrestrial OC
101 during land-ocean transfer. The age offset between lignin phenols and bulk OC was however
102 substantially higher in the three eastern GRARs (2,000 ^{14}C years) than in the three western

103 rivers (< 700 yr; Fig. 2b). As these estuarine sediments have all been shown to be dominated by
104 terrestrial OC with very minor contributions from rock-derived fossil carbon (26, 30), the larger age
105 offsets in eastern GRARs likely reflect the larger contribution of old OC from erosion of the loess-
106 like Yedoma ice complex that is prevalent in East Siberia (5, 13, 31).

107 Interestingly, the ^{14}C ages of lignin phenols were substantially younger than those of another
108 suite of terrestrial OC tracer compounds, i.e., long-chain higher plant leaf wax lipids (32) [$\text{C}_{27,29,31}$
109 *n*-alkanes and $\text{C}_{24,26,28}$ *n*-alkanoic acids ranging from 5500 to 13600 ^{14}C yr in age (6)] previously
110 measured in these sediment samples (Fig. 2b). The $\Delta^{14}\text{C}$ offset between lignin phenols and plant
111 wax lipids increased from ~160-180 ‰ in the continuous permafrost region (Kolyma and Indigirka)
112 to ~700 ‰ in the western watershed (Kalix) that has much lower permafrost coverage (Fig. 2a),
113 corresponding to a ^{14}C age offset of up to 13,000 yr (Fig. 2b). The sharply contrasting ^{14}C
114 characteristics suggest varied carbon sources and/or transfer mechanisms for these two groups of
115 higher plant markers. In contrast to lignin, which is enriched in woody debris and coarse soil
116 particles (33, 34), plant wax lipids are closely associated with fine-grained minerals and
117 preferentially stabilized in deep mineral soils (34). Therefore, while plant wax lipids constitute a
118 smaller component of the terrestrial OC (Table S2), their old ^{14}C ages reveal the mobilization of a
119 pre-aged (deep permafrost soil) carbon pool. By comparison, lignin phenols appear to trace
120 relatively recent OC inputs supplied from surface layers (organic and surface soil horizons).

121 Hydroxy phenols displayed another distinct pattern in their $\Delta^{14}\text{C}$ values across the transect,
122 with similar values to lignin phenols observed in two western rivers (-383 and +22 ‰ in Ob and
123 Kalix, respectively) and values lower than lignin phenols but comparable to plant wax lipids in the
124 three eastern GRARs (-529 to -477 ‰; Figs. 2b and S1b). Since wetlands dominated by *Sphagnum*
125 mosses constitute a high proportion of the Ob and Kalix basins (Table S1) (27, 28), hydroxy
126 phenols predominantly record OC inputs from contemporary wetlands in these watersheds and
127 hence bear a similar age to the surface OC pool (represented by lignin phenols). In contrast, East
128 Siberia has a very low wetland coverage (Fig. 2a and Table S1) but stores ancient peat deposits
129 enriched in hydroxy phenols in permafrost soils (2, 13). Such old carbon may be released through
130 cryoturbation, thermokarst and/or bank erosion processes (5, 35), contributing to the older ages of
131 hydroxy phenols relative to lignin phenols in eastern GRARs. These observations suggest that

132 hydroxy phenols incorporate carbon released from both surface and deep OC pools across the
133 transect.

134

135 **Hydrogeographic controls on the mobilization of different OC pools.** In accordance with the
136 above interpretations, mobilization of each carbon pool is mediated by different physiogeographic
137 and hydrological variables across the drainage basins (Figs. 2a and S2; Table S1). Among the
138 investigated physiogeographic variables, runoff exerts a strong control on the $\Delta^{14}\text{C}$ values of lignin
139 phenols across the Eurasian Arctic ($P < 0.01$; $R^2 = 0.92$; Figs. 3a) where younger lignin is
140 transported by rivers with a higher mean annual runoff rate. This correlation is consistent with the
141 efficient delivery of vascular plant debris during storm, flood and high-precipitation events (36-38),
142 suggesting increased transfer of surface detrital carbon in high-runoff systems. It is notable that at
143 zero runoff rate (representing extreme base flow with minimum detrital input), regression analysis
144 yields an end member $\Delta^{14}\text{C}$ value of -655 ‰ for lignin phenols, similar to that of plant wax lipids in
145 the westernmost (Kalix) estuary. Assuming that surface detrital carbon has decadal turnover times
146 in the high latitudes (39, 40), and hence a $\Delta^{14}\text{C}$ value of $+100$ to $+200 \text{ ‰}$, while deep soil-derived
147 lignin has a $\Delta^{14}\text{C}$ value of -655 ‰ , we estimate from a binary mixing model (Table S3) that ~30-90
148 % of mobilized lignin across the Eurasian Arctic reflects modern carbon sources.

149 In contrast, the $\Delta^{14}\text{C}$ values of plant wax lipids are most strongly correlated with the watershed
150 coverage of continuous permafrost ($P < 0.01$; $R^2 = 0.86$; Fig. 3b) but not with runoff ($P = 0.85$; Fig.
151 S2), consistent with enhanced mobilization of deep, old permafrost carbon in discontinuous
152 permafrost systems. This phenomenon may be associated with multiple processes. As continuous
153 permafrost shifts to more discontinuous or sporadic permafrost regimes westward in the transect,
154 more hydraulic conduits are accessible in the deep soil (Figs. 1b
155 carbon pools that are enriched in lipids relative to lignin. Moreover, thermokarst and thermal
156 erosion processes potentially increase from perennially-frozen regions to warmer, seasonally-frozen
157 zones (12, 41), enabling faster mobilization of deep OC from river banks and coastlines. While
158 erosion may also play a part in releasing lignin-rich OC from surface layers, its effect seems to be
159 dwarfed by surface runoff processes as neither temperature nor permafrost coverage is correlated
160 with the lignin age (Fig. S2). Hence, transport of younger lignin is enhanced in the river with the

-c), leading

161 highest runoff rate (Kalix; Fig. 2a), leading to a larger age offset between lignin phenols and plant
162 wax lipids towards the west end of the transect (Fig. 2b).

163 By comparison, corresponding $\Delta^{14}\text{C}$ values for hydroxy phenols were best correlated with the
164 wetland coverage in the drainage basin ($P < 0.01$; $R^2 = 0.86$; Fig. 3c), and to a lesser degree, with
165 the mean annual runoff rate ($P = 0.03$; $R^2 = 0.74$; Fig. 3d). This suggests that contemporary
166 wetlands are the main source of modern hydroxy phenols across the Eurasian Arctic, whose
167 delivery from surface litter and soil layers is, similar to lignin phenols, influenced by runoff
168 processes. Moreover, in the $\Delta^{14}\text{C}$ -runoff correlation plot (Fig. 3d), the hydroxy-phenol $\Delta^{14}\text{C}$ values
169 of four eastern rivers all fall below the general trend line (black line) and have a much flatter slope
170 against the runoff rate (blue line; $P < 0.05$; $R^2 = 0.81$). This suggests that surface runoff is less
171 efficient in supplying modern hydroxy phenols in the watersheds with a low wetland coverage,
172 where inputs of old hydroxy phenols from deeper soils are prominent.

173

174 **Contribution of surface and deep permafrost carbon to bulk sedimentary OC.** Our molecular
175 radiocarbon data show that detrital carbon from recent vegetation and surface organic layers is a key
176 component of the mobilized terrestrial carbon in the Eurasian Arctic that accumulates in estuarine
177 sediments. To evaluate the magnitude of permafrost-carbon release, we need to first assess the
178 contribution of surface and deep permafrost carbon pools to the bulk OC. Clearly, this is
179 complicated due to inputs from other organic components [such as black carbon (42, 43) and
180 planktonic carbon (5)], as underlined by the age difference of bulk OC relative to the terrestrial
181 markers in Lena, Ob and Yenisey sediments (Fig. 2b). Assuming that hydroxy phenols incorporate
182 the isotopic signal of terrestrial biospheric carbon derived from both surface and deep carbon
183 sources while the $\Delta^{14}\text{C}$ values of lignin phenols and plant wax lipids represent the integrated
184 radiocarbon signal of mobilized surface and deeper permafrost OC pools in each watershed,
185 respectively, we estimate from a binary mixing model that 47-77 % of terrestrial biospheric carbon
186 originates from deeper permafrost in the four eastern river basins (where modern wetland carbon
187 contribution is small; Table S4). This estimate likely represents a lower limit as the surface OC end
188 member (lignin) also incorporates a significant amount of pre-aged OC from surface soil horizons.
189 Nonetheless, it implies that over half of the sedimentary OC in East Siberian estuaries originates
190 from a previously stabilized or ancient soil pool, consistent with a recent estimate that 36-76 % of

191 sedimentary OC in the East Siberian Arctic Shelf is derived from erosion of Pleistocene Yedoma
192 (5).

193 During the second half of the twentieth century, Eurasian Arctic river runoff increased at an
194 average rate of approximately 0.60–0.74 mm/yr per year (44–46), likely increasing the delivery of
195 surface-derived OC into estuaries. Based on the relationship between lignin phenol $\Delta^{14}\text{C}$ values and
196 runoff ($\Delta^{14}\text{C} = 1.6018 \times \text{runoff} - 655$; Fig. 3a), the $\Delta^{14}\text{C}$ value of mobilized surface OC has
197 increased by approximately 19–24 ‰ from 1985 to 2004, not considering the variation of bomb-
198 derived ^{14}C in the atmosphere. This time window corresponds to the sediment-deposition time of 20
199 years, based on the surface sediment depth and sedimentation rate in the region (5). Assuming that
200 the ^{14}C signals of exported OC have remained similar during this period and that the endmember
201 $\Delta^{14}\text{C}$ value of deep permafrost OC has not altered, we estimate that the proportion of ancient OC in
202 the total terrestrial carbon pool has increased by 3–6% in four eastern GRAR sediments (Table S4)
203 over this period of time. When we assume that particulate organic carbon (POC) fluxes in these
204 rivers (Table S1) are dominantly terrestrial in origin (26, 30), the 20-year increase is equivalent to
205 approximately 1.4 Tg C transferred from old permafrost into estuarine sediments. While this
206 number represents a rough estimate and is relatively small as compared to some other Arctic carbon
207 fluxes (47), release of dissolved organic carbon (23, 47, 48) and water-column mineralization of
208 POC (5, 49) associated with permafrost thawing may well exceed the size of this sediment OC
209 budget in the context of a changing climate. Our estimate represents a conservative scenario as
210 sedimentary $\Delta^{14}\text{C}$ values are postulated to further decrease with warming. Furthermore, particle
211 transit time, albeit not well constrained, is likely to be longer than a few decades in these rivers,
212 given the residence time of suspended sediments in large meandering rivers [~ 17 kyr in the Amazon
213 River (50)] and woody debris in small mountainous rivers [~ 20 yr (51)]. The young terrestrial OC
214 components mobilized into these sediments from 1985 to 2004 were hence likely derived from
215 materials deposited in the surface layers before the 1980s and had an even larger increase in $\Delta^{14}\text{C}$
216 values due to the incorporation of bomb-derived ^{14}C into surface decadal OC pools (40). These
217 calculations suggest that the magnitude of permafrost-carbon release, which may be masked or
218 muted by other Arctic OC pools, is relevant on regional to continental scales.

219

220 **Implications for Arctic carbon cycling.** Our results reveal marked age offsets between different
221 terrestrial OC pools released from Arctic landscapes, which stands in contrast with some temperate
222 and tropical systems where terrestrial OC components are retained on land for a similar period of
223 time [such as the Columbia River (29)]. These findings highlight the linkage between carbon
224 cycling and hydrological processes, which is particularly close in Arctic landscapes where surface
225 and groundwater flows access different pools of carbon depending on the spatial distribution of
226 permafrost. Surface runoff appears to control the release of a major component of terrestrial carbon
227 while deep hydraulic conduits and bank/coastal erosion may mobilize very old permafrost carbon at
228 depth. This observation reveals an important caveat in deriving OC budgets or reconstructing past
229 carbon dynamics in the Arctic system based on bulk sedimentary OC properties as endmember
230 values may vary substantially due to the release of significantly pre-aged soil carbon. Molecular-
231 level ^{14}C measurements enable constraints to be placed on the relative contribution of surface and
232 deep permafrost carbon pools to Arctic fluvial export. Unravelling such hydrogeographic controls
233 on the differential delivery of Arctic carbon pools is key to unmasking warming effects on
234 permafrost-carbon release. As such, our data suggest that export of old deep permafrost OC as a
235 consequence of recent climate variations may be underestimated and masked by the synoptic
236 increase in the transport of young surface OC associated with enhanced river runoff in the Arctic.
237 The ability to differentiate and separately trace mobilized carbon pools across the Arctic will aid in
238 refining both our understanding of the contemporary system and our ability to predict linkages
239 between a warming climate and the mobilization of Arctic permafrost carbon.

240

241 **Materials and Methods**

242 **Study area.** The three eastern GRARs (Lena, Indigirka and Kolyma) drain into the Laptev Sea
243 (Lena) and the East Siberian Sea (Indigirka and Kolyma; Fig. 1a). The climate in the drainage basin
244 is semiarid to arid with average summer temperatures between +7 °C and +9 °C and winter
245 temperatures below -40 °C. This contrasts with the two western GRARs (Ob and Yenisey) located
246 in the west Siberian lowland and Kalix River that drains sub-Arctic Scandinavia into the Baltic Sea.
247 The drainage basins have average summer temperatures comparable to northeastern Eurasia but
248 much higher winter temperatures (around -20 °C) (28) and are wetter, with higher precipitation-to-
249 evaporation ratios compared to eastern GRARs. All rivers have comparable drainage-area-

250 normalized fluxes of total organic carbon (TOC) and POC (Table S1) (27, 52). A more detailed
251 description of the river drainage basins is provided elsewhere (26, 30). Surface sediments (0-2 cm)
252 were collected using a grab sampler from the GRAR estuaries during the second and third Russia-
253 United States cruises (on H/V Ivan Kireev) in 2004 and 2005 and from the Kalix in 2005 on the
254 research vessel “KBV005” from the Umeå Marine Research Center (UMF, Norrbyn, Sweden).
255 These sediments were mainly delivered by the annual spring freshet of the rivers and by coastal
256 erosion during the past ~20 years based on the sedimentation rate of 0.11-0.16 cm/yr (5, 26).
257 Previous molecular and isotopic investigations revealed a predominance of terrestrial OC with very
258 minor contributions from aquatic biomass or petrogenic (rock-derived) carbon into these estuarine
259 sediments (26, 30).

260

261 **Bulk analyses.** Bulk sediments were kept frozen at $-20\text{ }^{\circ}\text{C}$ after collection and freeze-dried prior to
262 analysis. A small aliquot was used for TOC and bulk $\delta^{13}\text{C}$ analyses at the UC Davis Stable Isotope
263 Facility (<http://stableisotopefacility.ucdavis.edu>) and for bulk $\Delta^{14}\text{C}$ analysis at the National Ocean
264 Sciences Accelerator Mass Spectrometry (NOSAMS) Facility at Woods Hole Oceanographic
265 Institution.

266

267 **Isolation and ^{14}C analysis of individual compounds.** As described previously (6), lipids were
268 extracted from freeze-dried sediments (~30-70 g) using soxhlet extraction with
269 dichloromethane/methanol (2:1; 24 h). Plant wax *n*-alkanes and *n*-alkanoic acids were isolated
270 using preparative capillary gas chromatography (PCGC) and analyzed for ^{14}C content. The solvent-
271 extracted residues were further hydrolyzed with 1 M KOH in methanol (100 $^{\circ}\text{C}$, 3 h) to remove
272 hydrolysable lipids. The dried residues were then subjected to alkaline CuO oxidation to release
273 lignin and hydroxy phenols on a microwave system (MARS, CEM Corporation) (53). For each
274 sample, approximately 5 g of CuO, 0.6 g of ferrous ammonium sulfate, and 25 mL of N_2 -bubbled
275 NaOH solution (2 M) were loaded into each of 5-8 vessels containing sediments (3-10 g) with ~50
276 mg of TOC. Vessels containing all reagents but no sample were also included as procedural blanks
277 along with each batch of sediments.

278 For compound-specific radiocarbon analysis, phenolic compounds were isolated using a high
279 pressure liquid chromatography (HPLC)-based method (SI Methods and details in ref. 29). Briefly,

280 the CuO oxidation extracts were purified through two solid phase extraction (SPE) cartridges
281 (Supelco Supelclean ENVI-18 and Supelclean LC-NH₂ SPEs) and separated through two HPLC-
282 isolation steps consisting of a Phenomenex Synergi Polar-RP column and a ZORBAX Eclipse
283 XDB-C18 column. Approximately 10-150 µg C of individual phenols were collected using a
284 fraction collector, yielding purities > 99%. Procedural blanks were processed in the same manner
285 for subsequent blank corrections.

286 Purified phenols were combusted under vacuum at 850 °C for 5 h. The resulting CO₂ was
287 cryogenically purified and quantified. A batch of CO₂ samples (~23-150 µg C) were sent to
288 NOSAMS, graphitized, and measured on accelerator mass spectrometry (AMS). A second batch of
289 CO₂ samples (~10-32 µg C) were directly measured without graphitization on the miniaturised
290 radiocarbon dating system (MICADAS) at ETH Zürich using a gas feeding system (54).
291 Radiocarbon contents are reported as Δ¹⁴C (‰) and conventional ¹⁴C age. Procedural blanks
292 associated with the extraction-HPLC-combustion procedures yielded 2.5 ± 0.8 µg C with an F_m
293 value of 0.21 ± 0.07 (n=5). All radiocarbon values are corrected for procedural blanks with the
294 errors propagated. We did not observe significant difference between radiocarbon contents of the
295 same sample measured at the two AMS facilities.

296

297 **Binary mixing model.** We employed a ¹⁴C binary mixing model to assess the relative contributions
298 of surface OC (Table S3) and permafrost OC (Table S4) to lignin or hydroxy phenols, respectively.
299 The model is expressed in the following two equations:

$$300 \quad f_S (\Delta^{14}C_S) + f_P (\Delta^{14}C_P) = \Delta^{14}C_{\text{phenol}} \quad [1]$$

$$301 \quad f_S + f_P = 1 \quad [2]$$

302 where f is the percentage of surface or permafrost OC and the subscripts S and P refer to surface
303 and permafrost, respectively.

304

305 **Modeling and statistical analysis.** A T test was used to compare the ¹⁴C content of different
306 phenols. Differences are considered to be significant at a level of $P < 0.05$. Linear regression
307 analysis was used to assess the correlation between drainage basin characteristics and the ¹⁴C
308 content of terrestrial OC markers (Fig. S2). The main drainage basin parameters investigated as
309 explanatory variables include basin area, runoff rate, mean annual summer cumulative temperature

310 (ASCT) and the coverage of forest, wetland and continuous permafrost in the watershed (Table S1).
311 ASCT is calculated as the sum of mean monthly temperature for months with a mean temperature
312 above 0°C within a year (details in SI Methods and Fig. S3) and is considered to have a major
313 impact on permafrost thawing (55). POC flux and discharge are found to be correlated with
314 continuous permafrost coverage ($P < 0.05$; $R^2 = 0.85$) and basin area ($P < 0.05$; $R^2 = 0.84$)
315 respectively, and are hence not included as basin parameters in the ^{14}C correlation analyses.
316 Correlation is considered to be significant at a level of $P < 0.05$ and the R^2 values are used to
317 compare the explanatory power of the variables.

318

319 **Acknowledgments**

320 We thank all colleagues in the International Siberian Shelf Study (ISSS) Program for support
321 including sampling. We thank Li Xu for assistance with AMS analyses at WHOI. Christopher
322 Reddy is acknowledged for providing access to an HPLC system. The ISSS program is supported
323 by the Knut and Alice Wallenberg Foundation, the Far Eastern Branch of the Russian Academy of
324 Sciences, the Swedish Research Council, the US National Oceanic and Atmospheric Administration,
325 the Russian Foundation of Basic Research, the Swedish Polar Research Secretariat and the Nordic
326 Council of Ministers (Arctic Co-Op and TRI-DEFROST programs). Ö.G. acknowledges an
327 Academy Research Fellow grant from the Swedish Royal Academy of Sciences. Grants OCE-
328 9907129, OCE-0137005, and OCE-0526268 from the US National Science Foundation (NSF), the
329 Stanley Watson Chair for Excellence in Oceanography (to T.I.E.) and ETH Zürich enabled this
330 research. J.E.V. thanks support from NWO-Rubicon (#825.10.022). B.E.v.D thanks support from
331 the UK NERC (NE/I024798/1). X.F. thanks WHOI for a postdoctoral scholar fellowship and for
332 postdoctoral support from ETH Zürich.

333

334 **Author Contributions**

335 X.F., T.I.E. and Ö.G. conceived the idea of using molecular ^{14}C analyses to deconvolute
336 environmental effects on the release of terrestrial carbon pools across Eurasian Arctic. J.E.V.,
337 B.E.v.D., Ö.G., I.P.S. and O.V.D. collected samples. B.E.v.D. and J.E.V. prepared samples for bulk
338 organic carbon analyses, stable isotope analysis and radiocarbon analyses (sediments). X.F.
339 conducted compound-specific radiocarbon analysis of lignin and hydroxy phenols with assistance of

340 D.B.M. Radiocarbon analyses were facilitated by T.I.E. Z.W. and X.F. performed modeling and
341 data analyses. X.F. wrote the paper, with input from all other authors.

342

343 **References**

- 344 1. Tarnocai C, et al. (2009) Soil organic carbon pools in the northern circumpolar permafrost
345 region. *Global Biogeochem Cy* 23, GB2023, 2010.1029/2008GB003327.
- 346 2. Schuur EAG, et al. (2008) Vulnerability of permafrost carbon to climate change: Implications
347 for the global carbon cycle. *Bioscience* 58(8):701-714.
- 348 3. Dorrepaal E, et al. (2009) Carbon respiration from subsurface peat accelerated by climate
349 warming in the subarctic. *Nature* 460:616-619.
- 350 4. Schuur EAG, et al. (2009) The impact of permafrost thaw on old carbon release and net carbon
351 exchange from tundra. *Nature* 459:556-559.
- 352 5. Vonk JE, et al. (2012) Activation of old carbon by erosion of coastal and subsea permafrost in
353 Arctic Siberia. *Nature* 489:137-140.
- 354 6. Gustafsson Ö, van Dongen BE, Vonk JE, Dudarev OV, Semiletov IP (2011) Widespread
355 release of old carbon across the Siberian Arctic echoed by its large rivers. *Biogeosciences*
356 8:1737-1743.
- 357 7. Schaefer K, Zhang T, Bruhwiler L, Barrett AP (2011) Amount and timing of permafrost carbon
358 release in response to climate warming. *Tellus* 63B:165-180.
- 359 8. Guo L, Ping CL, Macdonald RW (2007) Mobilization pathways of organic carbon from
360 permafrost to Arctic rivers in a changing climate. *Geophys Res Lett* 34, L13603,
361 13610.11029/12007GL030689.
- 362 9. Holmes RM, et al. (2013) in *Climatic Change and Global Warming of Inland Waters: Impacts*
363 *and Mitigation for Ecosystems and Societies*, eds Goldman CR, Kumagai M, Robarts RD (John
364 Wiley & Sons, Ltd), pp 3-26.
- 365 10. Charkin AN, et al. (2011) Seasonal and interannual variability of sedimentation and organic
366 matter distribution in the Buor-Khaya Gulf: the primary recipient of input from Lena River and
367 coastal erosion in the southeast Laptev Sea. *Biogeosciences* 8:2581-2594.
- 368 11. Semiletov IP, Shakhova NE, Sergienko VI, Pipko II, Dudarev OV (2012) On carbon transport
369 and fate in the East Siberian Arctic land-shelf-atmosphere system. *Environ Res Lett* 7, 015201,
370 10.1088/1748-9326/7/1/015201.

- 371 12. Costard F, et al. (2007) Impact of the global warming on the fluvial thermal erosion over the
372 Lena River in central Siberia. *Geophys Res Lett* 34, L14501, 10.1029/2007GL030212.
- 373 13. Schirrmeister L, et al. (2011) Fossil organic matter characteristics in permafrost deposits of the
374 northeast Siberian Arctic. *J Geophys Res* 116, G00M02, 10.1029/2011JG001647.
- 375 14. Raymond PA, Bauer JE (2001) Riverine export of aged terrestrial organic matter to the North
376 Atlantic Ocean. *Nature* 409:497-500.
- 377 15. Guo L, Macdonald RW (2006) Source and transport of terrigenous organic matter in the upper
378 Yukon River: Evidence from isotope ($\delta^{13}\text{C}$, $\Delta^{14}\text{C}$, and $\delta^{15}\text{N}$) composition of dissolved,
379 colloidal, and particulate phases. *Global Biogeochem Cy* 20, GB2011,
380 10.1029/2005GB002593.
- 381 16. Kusch S, Rethemeyer J, Schefuss E, Mollenhauer G (2010) Controls on the age of vascular
382 plant biomarkers in Black Sea sediments. *Geochim Cosmochim Acta* 74(24):7031-7047.
- 383 17. Karlsson ES, et al. (2011) Carbon isotopes and lipid biomarker investigation of sources,
384 transport and degradation of terrestrial organic matter in the Buor-Khaya Bay, SE Laptev Sea.
385 *Biogeosciences* 8:1865-1879.
- 386 18. Dickens AF, Baldock J, Kenna TC, Eglinton TI (2011) A depositional history of particulate
387 organic carbon in a floodplain lake from the lower Ob' River, Siberia. *Geochim Cosmochim*
388 *Acta* 75:4796-4815.
- 389 19. Vonk JE, et al. (2010) Molecular and radiocarbon constraints on sources and degradation of
390 terrestrial organic carbon along the Kolyma paleoriver transect, East Siberian Sea.
391 *Biogeosciences* 7:3153-3166.
- 392 20. Hedges JI, Keil RG, Benner R (1997) What happens to terrestrial organic matter in the ocean?
393 *Org Geochem* 27(5/6):195-212.
- 394 21. Hugelius G, Kuhry P (2009) Landscape partitioning and environmental gradient analyses of
395 soil organic carbon in a permafrost environment. *Global Biogeochem Cy* 23, GB3006,
396 10.102912008GB102003419.
- 397 22. Vonk JE, Gustafsson Ö (2009) Calibrating *n*-alkane Sphagnum proxies in sub-Arctic
398 Scandinavia. *Org Geochem* 40:1085-1090.
- 399 23. Amon RMW, et al. (2012) Dissolved organic matter sources in large Arctic rivers. *Geochim*
400 *Cosmochim Acta* 94:217-237.

- 401 24. Lehto O, Tuhkanen M, Ishiwatari R, Uzaki M (1985) Quantitative gas chromatographic
402 analysis of degradation and oxidation products from a Finnish *Sphagnum* peat. *Suo (Helsinki)*
403 36:101-106.
- 404 25. Zaccone C, Said-Pullicino D, Gigliotti G, Miano TM (2008) Diagenetic trends in the phenolic
405 constituents of *Sphagnum*-dominated peat and its corresponding humic acid fraction. *Org*
406 *Geochem* 39:830-838.
- 407 26. van Dongen BE, Semiletov I, Weijers JWH, Gustafsson Ö (2008) Contrasting lipid biomarker
408 composition of terrestrial organic matter exported from across the Eurasian Arctic by the five
409 great Russian Arctic rivers. *Global Biogeochem Cy* 22, GB1011, 10.1029/2007GB002974.
- 410 27. Ingri J, Widerlund A, Land M (2005) Geochemistry of major elements in a pristine boreal river
411 system; hydrological compartments and flow paths. *Aquat Geochem* 11:57-88.
- 412 28. Kremenetski KV, et al. (2003) Peatlands of the western Siberian lowlands: Current knowledge
413 on zonation, carbon content and Late Quaternary history. *Quaternary Sci Rev* 22:703-723.
- 414 29. Feng X, et al. (2013) ¹⁴C and ¹³C characteristics of higher plant biomarkers in Washington
415 margin surface sediments. *Geochim Cosmochim Acta* 105:14-30.
- 416 30. Vonk JE, van Dongen BE, Gustafsson Ö (2008) Lipid biomarker investigation of the origin and
417 diagenetic state of sub-arctic terrestrial organic matter presently exported into the northern
418 Bothnian Bay. *Mar Chem* 112:1-10.
- 419 31. Romanovskii NN (1993) *Fundamentals of the Cryogenesis of the Lithosphere* (Moscow
420 University Press, Moscow).
- 421 32. Harwood JL, Russell NJ (1984) *Lipids in Plants and Microbes* (George Allen & Unwin,
422 London).
- 423 33. Wakeham SG, et al. (2009) Partitioning of organic matter in continental margin sediments
424 among density fractions. *Mar Chem* 115:211-225.
- 425 34. Xu C, Guo L, Ping CL, White DM (2009) Chemical and isotopic characterization of size-
426 fractionated organic matter from cryoturbated tundra soils, northern Alaska. *J Geophys Res*
427 114, G03002, 10.1029/2008JG000846.
- 428 35. Semiletov IP, et al. (2011) Carbon transport by the Lena River from its headwaters to the
429 Arctic Ocean, with emphasis on fluvial input of terrestrial particulate organic carbon vs. carbon
430 transport by coastal erosion. *Biogeosciences* 8:2407-2426.
- 431 36. Hilton RG, et al. (2008) Tropical-cyclone-driven erosion of the terrestrial biosphere from
432 mountains. *Nat Geosci* 1:759-762.

- 433 37. Leithold EL, Hope RS (1999) Deposition and modification of a flood layer on the northern
434 California shelf: lessons from and about the fate of terrestrial particulate organic carbon. *Mar*
435 *Geol* 154:183-195.
- 436 38. Smith JC, et al. (2013) Runoff-driven export of particulate organic carbon from soil in
437 temperate forested uplands. *Earth Planet Sci Lett* 365:198-208.
- 438 39. Bird MI, Chivas AR, Head J (1996) A latitudinal gradient in carbon turnover times in forest
439 soils. *Nature* 381:143-146.
- 440 40. Fröberg M, Tipping E, Stendahl J, Clarke N, Bryant C (2011) Mean residence time of O
441 horizon carbon along a climatic gradient in Scandinavia estimated by ^{14}C measurements of
442 archived soils. *Biogeochemistry* 104:227-236.
- 443 41. Toniolo H, Kodial P, Hinzman LD, Yoshikawa K (2009) Spatio-temporal evolution of a
444 thermokarst in Interior Alaska. *Cold Reg Sci Technol* 56:39-49.
- 445 42. Elmquist M, Semiletov I, Guo L, Gustafsson Ö (2008) Pan-Arctic patterns in black carbon
446 sources and fluvial discharges deduced from radiocarbon and PAH source apportionment
447 markers in estuarine surface sediments *Global Biogeochem Cy* 22, GB2018,
448 2010.1029/2007GB002994.
- 449 43. Guo L, et al. (2004) Characterization of Siberian Arctic coastal sediments: Implications for
450 terrestrial organic carbon export. *Global Biogeochem Cy* 18, GB1036,
451 1010.1029/2003GB002087.
- 452 44. McClelland JW, Dery SJ, Peterson BJ, Holmes RM, Wood EF (2006) A pan-arctic evaluation
453 of changes in river discharge during the latter half of the 20th century. *Geophys Res Lett* 33,
454 L06715, 10.1029/2006GL025753.
- 455 45. Peterson BJ, et al. (2002) Increasing river discharge to the Arctic Ocean. *Science* 298:2171-
456 2173.
- 457 46. Savelieva NI, Semiletov IP, Vasilevskaya LN, Pugach SP (2000) A climate shift in seasonal
458 values of meteorological and hydrological parameters for Northeastern Asia. *Prog Oceanogr*
459 47:279-297.
- 460 47. Dittmar T, Kattner G (2003) The biogeochemistry of the river and shelf ecosystem of the
461 Arctic Ocean: a review. *Mar Chem* 83:103-120.
- 462 48. Lobbes JM, Fitznar HP, Kattner G (2000) Biogeochemical characteristics of dissolved and
463 particulate organic matter in Russian rivers entering the Arctic Ocean. *Geochim Cosmochim*
464 *Acta* 64:2973-2983.

- 465 49. Sánchez-García L, et al. (2011) Inventories and behavior of particulate organic carbon in the
466 Laptev and East Siberian seas. *Global Biogeochem Cy* 25, GB2007,
467 2010.1029/2010GB003862.
- 468 50. Dosseto A, Bourdon B, Gaillardet J, Maurice-Bourgoin L, Allègre CJ (2006) Weathering and
469 transport of sediments in the Bolivian Andes: Time constraints from uranium-series isotopes.
470 *Earth Planet Sci Lett* 248(3-4):759-771.
- 471 51. Hyatt TL, Naiman RJ (2001) The residence time of large woody debris in the Queets River,
472 Washington, USA. *Ecol Appl* 11(1):191-202.
- 473 52. Stein R, Macdonald RW (2004) *The Organic Carbon Cycle in the Arctic Ocean* (Springer,
474 Berlin).
- 475 53. Goñi MA, Montgomery S (2000) Alkaline CuO oxidation with a microwave digestion system:
476 Lignin analyses of geochemical samples. *Anal Chem* 72(14):3116-3121.
- 477 54. Wacker L, et al. (2013) A versatile gas interface for routine radiocarbon analysis with a gas ion
478 source. *Nucl Instr Meth Phys Res B* 294:315-319.
- 479 55. Rinke A, et al. (2012) Arctic RCM simulations of temperature and precipitation derived indices
480 relevant to future frozen ground conditions. *Global Planet Change* 80-81:136-148.
- 481

482

483 **Figure Legends**

484 **Figure 1:** The Eurasian Arctic transect and cartoon of hydrological mobilization of terrestrial
485 carbon into rivers. (a) Map of the rivers (black lines) with permafrost distribution (modified from
486 refs. 1 and 6) and sampling locations (red circles); (b) illustration of the western Eurasian Arctic
487 characterized by extensive moss-dominated wetlands underlain by discontinuous permafrost and
488 ubiquitous deep groundwater conduits; (c) illustration of eastern Eurasian Arctic characterized by a
489 wide distribution of Yedoma ice complex, a thin seasonally thawing active layer and thick
490 continuous permafrost below. Blue arrows indicate hydrological transport of carbon from different
491 physiogeographic regimes.

492

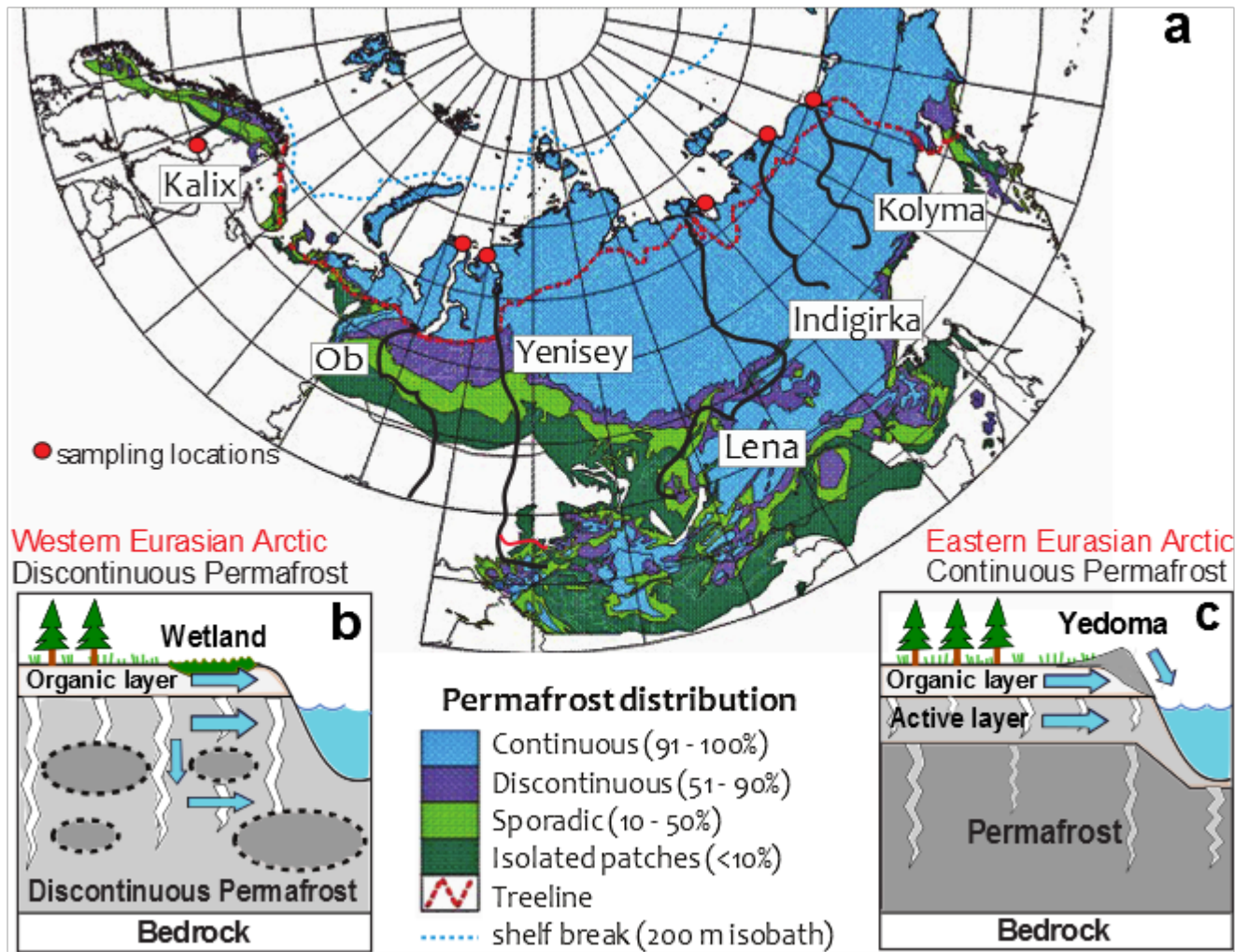
493 **Figure 2:** Hydrogeographic characteristics of the Eurasian Arctic rivers (a) and contrasting
494 radiocarbon contents (expressed as $\Delta^{14}\text{C}$ and conventional ^{14}C age) of terrestrial markers as
495 compared with bulk organic carbon (OC) in the estuarine surface sediments (b). Runoff rate =
496 discharge/basin area. Detailed hydrogeographic data are listed in Table S1 [compiled from refs. 6,
497 9, 27, 52 and "watersheds of the world" (<http://archive.wri.org>)]. The $\Delta^{14}\text{C}$ values of terrestrial
498 markers represent concentration-weighted averages with the standard errors of analytical
499 measurement propagated. Lignin phenols refer to vanillyl and syringyl phenols (detailed data in Fig.
500 S1). Hydroxy phenols refer to *p*-hydroxybenzaldehyde, *p*-hydroxyacetophenone and *p*-
501 hydroxybenzoic acid. Plant wax lipids constitute *n*-alkanes ($\text{C}_{27,29,31}$) and *n*-alkanoic acids ($\text{C}_{24,26,28}$)
502 (6).

503

504 **Figure 3:** Hydrological and physiogeographic controls on the age of terrestrial markers in the
505 integrating Eurasian Arctic estuaries: correlation of (a) $\Delta^{14}\text{C}_{\text{lignin phenols}}$ with runoff rate; (b) $\Delta^{14}\text{C}_{\text{plant}}$
506 wax lipids with continuous permafrost coverage; (c) $\Delta^{14}\text{C}_{\text{hydroxy phenols}}$ with wetland coverage; (d)
507 $\Delta^{14}\text{C}_{\text{hydroxy phenols}}$ with runoff rate. The blue dotted line in (d) represents linear correlation for the data
508 of four eastern rivers ($P < 0.05$; $R^2 = 0.81$). *Runoff rate = discharge/basin area. Contents of
509 terrestrial markers are defined in Fig. 2. Further statistical analyses can be found in Fig. S2.

510

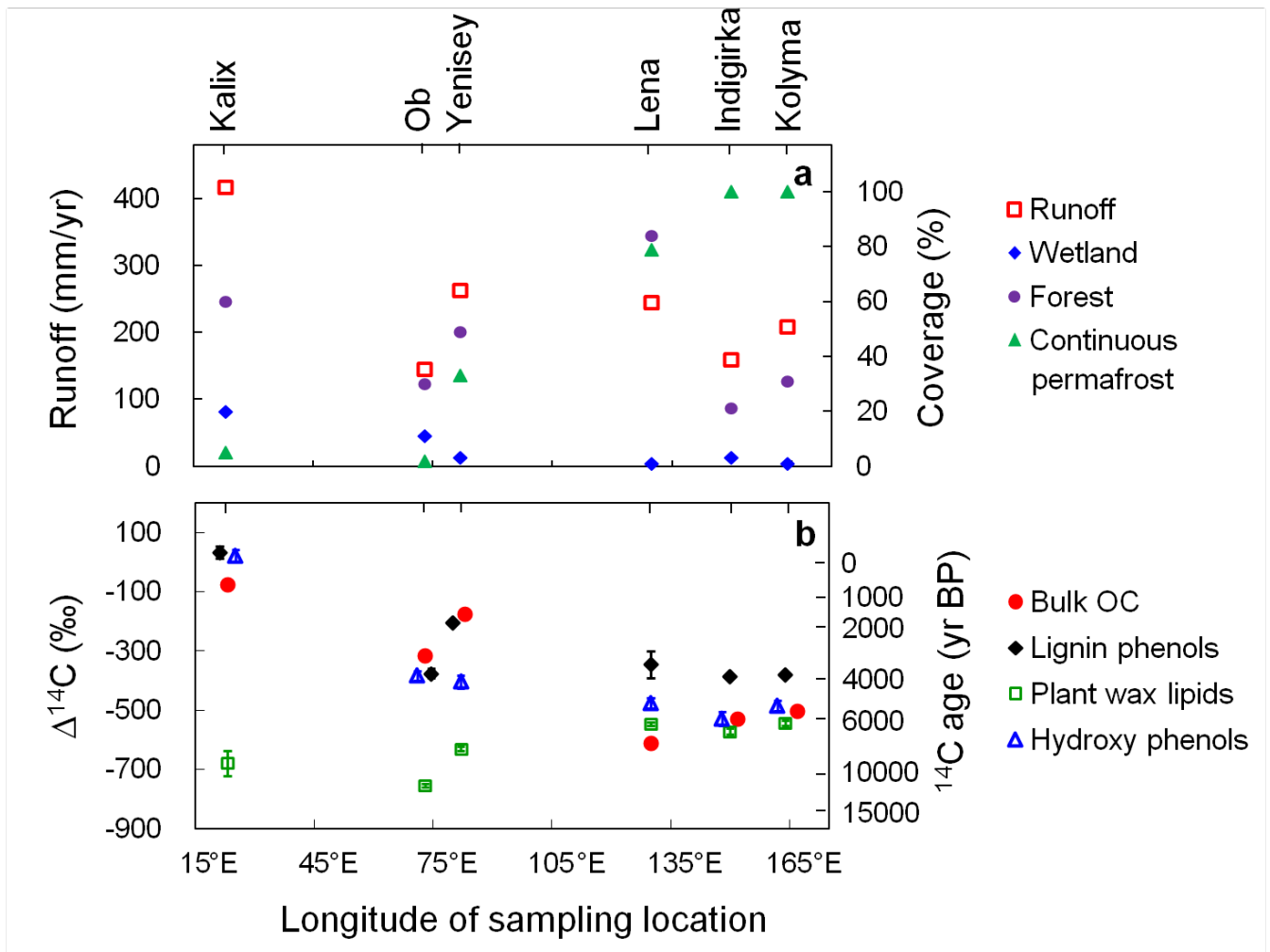
511 Figure 1



512

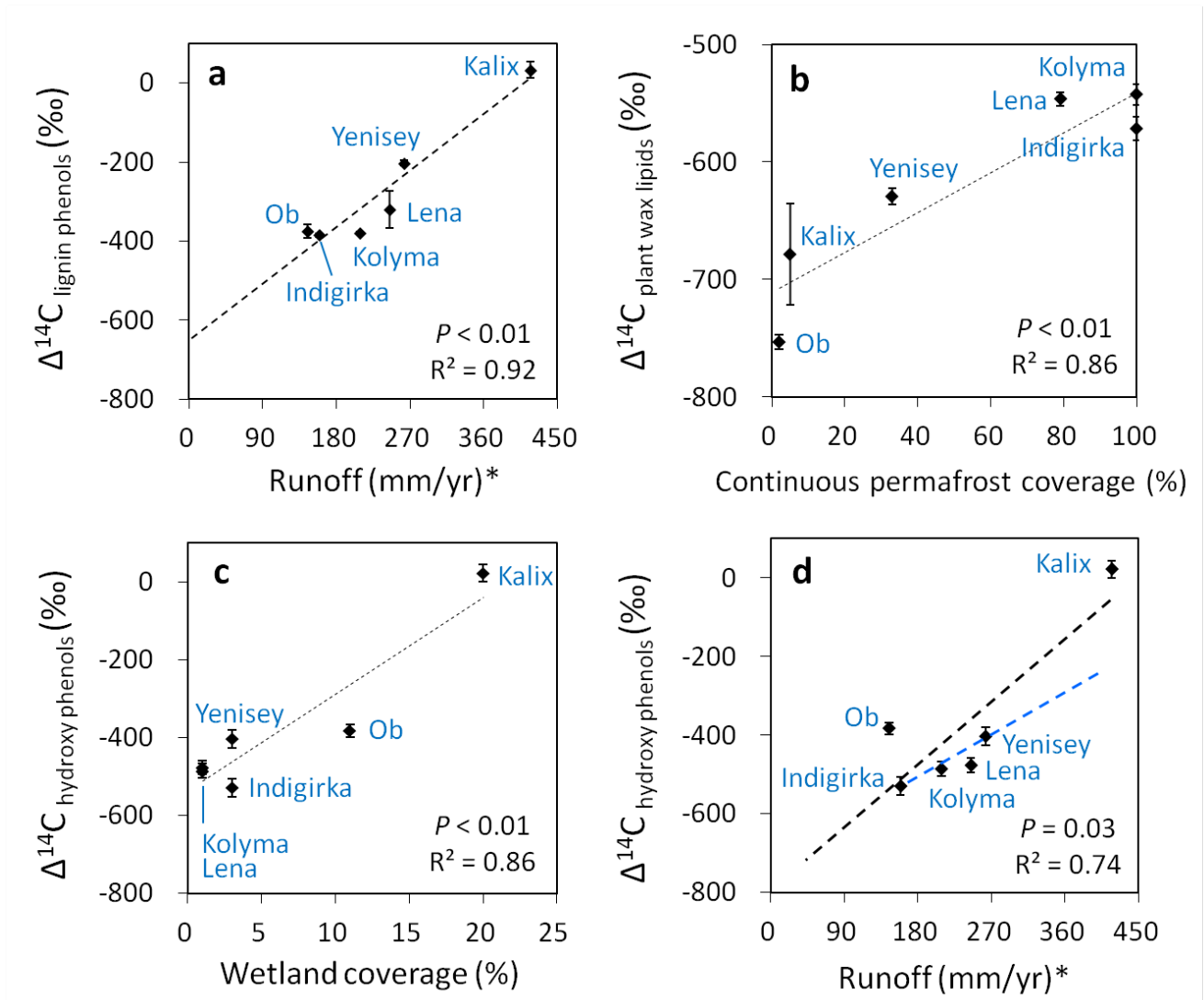
513

514 Figure 2



515

516



Supporting Information

SI Methods

Isolation of lignin phenols for ^{14}C analysis. Details of the method are provided in ref. (1). Briefly, the CuO oxidation products (in ethyl acetate) were blown carefully to $< 100\ \mu\text{L}$ under N_2 , re-dissolved in water (pH 2) and loaded onto a Supelclean ENVI-18 solid phase extraction (SPE) cartridge (Supelco, pre-conditioned with methanol and water). Lignin oxidation products were eluted with acetonitrile from the ENVI-18 SPE cartridge, blown under N_2 to a volume of $< 0.5\ \text{mL}$ and further separated on a self-packed amino SPE cartridge (0.5 g, Supelclean LC- NH_2 , Supelco, preconditioned with methanol) into phenolic aldehyde/ketone (eluting in methanol) and their corresponding acid (eluting with methanol:12 M HCl, 95:5) fractions. Each fraction was blown carefully to $< 100\ \mu\text{L}$ under N_2 and re-dissolved in methanol for separation on an Agilent 1200 HPLC system coupled to a diode array detector (DAD) and a fraction collector. Individual phenols were collected through two HPLC-isolation steps consisting of a Phenomenex Synergi Polar-RP column (4 μm ; 4.6 \times 250 mm) with a Polar-RP SecurityGuard column (4 μm ; 4.0 \times 3.0 mm) and a ZORBAX Eclipse XDB-C18 column (5 μm ; 4.6 \times 150 mm) with a ZORBAX Eclipse C18 guard column (5 μm ; 4.6 \times 12.5 mm). The column temperature was maintained at 28 $^\circ\text{C}$ and a binary gradient of water/acetic acid (99.8:0.2) and methanol/acetonitrile (50:50) was used as mobile phases (flow rate of 0.8 mL/min; details in ref. 1). A total of 5 injections (in most cases; and 10 injections for phenols $> 150\ \mu\text{g}$) were conducted for each sample to collect approximately 20-300 μg of each phenol (i.e., $\sim 10\text{--}150\ \mu\text{g C}$) for ^{14}C measurement. After isolation, phenols were recovered from the aqueous mobile phase through extraction with ethyl acetate at pH 2 and eluted from a 5% deactivated SiO_2 column using ethyl acetate to remove potential column bleed. A small aliquot of purified phenols was derivatized with N,O-bis-(trimethylsilyl) trifluoroacetamide (BSTFA) and pyridine to check compound purity by gas chromatography-mass spectrometry, and was found to yield purities $> 99\%$. Purified phenols were transferred into pre-combusted quartz tubes in ethyl acetate and blown dry carefully under a gentle stream of N_2 , with the addition of pre-combusted CuO afterwards. The quartz tubes were evacuated on a vacuum line while immersed in an isopropanol/dry ice slush ($-78\ ^\circ\text{C}$), flame sealed, and combusted at 850 $^\circ\text{C}$ for 5 h. The resulting CO_2 was cryogenically purified and quantified by expansion into a calibrated volume. The procedural blanks were processed in the same manner.

32

33 **Regional temperature data.** Mean monthly temperatures (T_m) recorded at climatic stations in
34 the six watersheds (Fig. S3) from 1955 to 2004 were obtained from the Global Historical
35 Climatology Network Monthly (GHCN-M, v.3; <http://www.ncdc.noaa.gov/ghcnm/>). In total, 102
36 climatic stations were identified within the GRAR watersheds (Fig. S3). No climatic station
37 within the Kalix drainage basin was found in the GHCN-M database. The five closest stations
38 within 110 km from the watershed boundary were hence selected. Similarly, GHCN-M database
39 recorded only two climate stations within the Indigirka watershed. To increase the reliability of
40 the Indigirka climatic data, we selected another three stations within 250 km from the watershed
41 boundary.

42 We used annual summer cumulative temperature (ASCT) as a key temperature variable
43 because summer temperatures are considered to have a major impact on permafrost thawing (2)
44 and experience more variations than mean annual temperature (MAT) during recent climate
45 change (3). The value of ASCT is given by the sum of mean monthly temperatures (T_m) for
46 months with a T_m above 0°C each year and is thus related to the “thawing index” (4). ASCT
47 from 1985 to 2004 was calculated for each station separately and then averaged to represent the
48 entire watershed.

SI Tables

Table S1: Sample location, drainage basin characteristics and bulk sediment properties of the Great Russian Arctic Rivers (GRARs) and Kalix River

	Kalix	Ob	Yenisey	Lena	Indigirka	Kolyma
Latitude; Longitude	65.44°N; 23.20°E	72.65°N; 73.44°E	72.61°N; 79.86°E	71.96°N; 129.54°E- 71.02°N; 132.60°E*	72.06°N; 150.46°E	70.00°N; 163.70°E
Geological and physiographic regions [†]	Scandinavian mountains	West Siberian lowlands	West Siberian lowlands	Central Siberian plateau	East Siberian highlands	East Siberian highlands
Mean ASCT (1985 ± 2004; °C)	53.7	87.4	65.4	57.9	40.7	47.9
Forest coverage (%) [§]	60	30	49	84	21	31
Wetland coverage (%) [§]	20	11	3	1	3	1
Permafrost coverage [¶]	5/15/80	2/24/74	33/55/12	79/20/1	100/0/0	100/0/0
Basin area (10 ⁶ km ²)	0.024	2.54-2.99	2.44-2.59	2.40-2.49	0.34-0.36	0.65-0.66
Discharge (km ³ /yr) ^{**}	10	427	673	588	54	136
Runoff (mm/yr) ^{**}	417	145	263	245	159	209
TOC/POC flux (t km ⁻² yr ⁻¹) ^{††}	1.4/0.099	1.1/0.14	1.8/0.066	1.9/0.49	1.2/0.47	1.5/0.48
OC (%)	4.5	0.9	1.9	0.5	1.5	1.7
OC/N ^{‡‡}	10.9 ± 0.3	10.0 ± 0.1	10.5 ± 0.1	12.3 ± 0.8	14.7 ± 0.2	15.9 ± 1.2
δ ¹³ C-TOC (‰)	-27.1	-27.4	-26.5	-25.0	-26.6	-26.7
Δ ¹⁴ C-TOC (‰) ^{§§}	-74 ± 37	-314 ± 3	-175 ± 3	-609 ± 3	-527 ± 3	-502 ± 2
¹⁴ C age of TOC (yr BP) ^{§§}	570 ± 250	3000 ± 35	1500 ± 30	7500 ± 60	6000 ± 50	5600 ± 50

* Combined surface sediments along a transect;

† According to ref. (5);

‡ ASCT: annual summer cumulative temperature, calculated as the sum of mean monthly temperature for months with a mean temperature above 0°C within a year, temperature data derived from the Global Historical Climatology Network Monthly (GHCN-M) database.

§ Data from ref. (6) and "Watersheds of the world" (<http://archive.wri.org>);

¶ Given as % continuous; % (discontinuous+sporadic+isolated); % non-permafrost (7, 8);

|| Data from refs. (6, 9-11);

** Data from refs. (6, 8, 12);

†† Kalix data from ref. (6), GRAR data from ref. (12);

‡‡ Mass ratio of OC to total nitrogen (13, 14);

§§ Measured in 2006; values normalized for the year of measurement; BP: before present.

Table S2: Abundance of terrestrial OC markers in the estuarine surface sediments (mg/g OC) of the Great Russian Arctic Rivers (GRARs) and Kalix River

	Kalix	Ob	Yenisey	Lena	Indigirka	Kolyma
Lignin phenols*	14.35	13.36	11.15	11.41	21.37	22.78
vanillin	4.06	3.11	2.94	3.64	4.58	5.17
acetovanillone	2.04	1.80	1.76	2.30	3.68	3.38
vanillic acid	2.34	2.35	2.38	2.78	3.62	3.69
syringaldehyde	1.73	2.51	1.75	1.13	3.90	4.20
acetosyringone	0.75	1.06	0.58	0.32	1.55	1.75
syringic acid	1.42	1.45	0.87	0.67	2.16	2.60
<i>p</i> -coumaric acid	1.60	0.56	0.52	0.40	0.78	0.93
ferulic acid	0.41	0.52	0.34	0.18	1.11	1.05
Hydroxy phenols*	6.73	4.13	2.90	3.67	4.37	4.80
<i>p</i> -hydroxybenzaldehyde	2.92	1.02	0.75	0.99	0.90	0.93
<i>p</i> -hydroxyacetophenone	1.32	0.75	0.43	0.50	0.44	0.81
<i>p</i> -hydroxybenzoic acid	2.49	2.36	1.72	2.18	3.03	3.06
Plant wax lipids[†]	0.44	0.91	0.62	0.44	1.22	1.17
C _{27,29,31} <i>n</i> -alkanes [†]	0.16	0.76	0.48	0.28	0.91	0.65
C _{24,26,28} <i>n</i> -alkanoic acids [†]	0.28	0.15	0.14	0.16	0.31	0.52

* Lignin and hydroxy phenols were measured on GC/MS as trimethylsilyl derivatives of CuO oxidation products;

[†] Plant wax lipids refer to the summary of C_{27,29,31} *n*-alkanes and C_{24,26,28} *n*-alkanoic acids measured previously (13, 14).

Table S3: Average $\Delta^{14}\text{C}$ values of lignin phenols in estuarine surface sediments of the Great Russian Arctic Rivers (GRARs) and Kalix River and contributions of modern surface OC to lignin estimated from the ^{14}C binary mixing model

	Kalix	Ob	Yenisey	Lena	Indigirka	Kolyma
Average $\Delta^{14}\text{C}$ of lignin phenols (‰) [*]	+33 ± 21	-375 ± 17	-203 ± 7	-320 ± 46	-385 ± 4	-379 ± 3
Percentage of modern surface OC in lignin (%)						
When $\Delta^{14}\text{C}_\text{S} = +100$ ‰, $\Delta^{14}\text{C}_\text{P} = -655$ ‰ [†]	91 ± 3	37 ± 2	60 ± 1	44 ± 6	36 ± 1	37 ± 1
When $\Delta^{14}\text{C}_\text{S} = +200$ ‰, $\Delta^{14}\text{C}_\text{P} = -655$ ‰ [†]	80 ± 3	33 ± 2	53 ± 1	39 ± 6	32 ± 1	32 ± 1

* Abundance-weighted average values with errors propagated, original values in Fig. S1;

† $\Delta^{14}\text{C}_\text{S}$ and $\Delta^{14}\text{C}_\text{P}$ refer to the $\Delta^{14}\text{C}$ value of surface and permafrost OC, respectively; the $\Delta^{14}\text{C}_\text{P}$ value is estimated from the regression relationship between lignin phenol $\Delta^{14}\text{C}$ values and runoff rate (Fig. 3a).

Table S4: Average $\Delta^{14}\text{C}$ values of terrestrial OC pools (represented by different groups of markers) and contributions of surface versus deep permafrost OC to terrestrial biospheric OC in surface sediments of the Great Russian Arctic Rivers (GRARs) and Kalix River in 2004 and 1985

	Kalix	Ob	Yenisey	Lena	Indigirka	Kolyma
Average $\Delta^{14}\text{C}$ value of terrestrial biospheric OC (represented by hydroxy phenols)*	+22 ± 22	-383 ± 15	-404 ± 23	-477 ± 18	-529 ± 23	-486 ± 18
<i>Current budget (2004)</i>						
Average $\Delta^{14}\text{C}$ value of terrestrial OC pools (‰)						
Surface-dominated OC (represented by lignin phenols)*	+33 ± 21	-375 ± 17	-203 ± 7	-320 ± 46	-385 ± 4	-379 ± 3
Deep-permafrost-dominated OC (represented by plant wax lipids)†	-679 ± 43	-753 ± 6	-630 ± 7	-546 ± 6	-571 ± 10	-543 ± 9
Contribution of OC pools (%)‡						
Surface OC	98 ± 2	98 ± 2	53 ± 5	31 ± 8	23 ± 13	35 ± 11
Deep permafrost OC	2 ± 2	2 ± 2	47 ± 5	69 ± 8	77 ± 13	65 ± 11
<i>Budget of the past (1985)</i>						
Average $\Delta^{14}\text{C}$ value of terrestrial OC pools (‰)						
Surface-dominated OC (represented by lignin phenols)§	+9 ± 21	-399 ± 17	-227 ± 7	-344 ± 46	-404 ± 4	-403 ± 3
Deep-permafrost-dominated OC (represented by plant wax lipids)§	-679 ± 43	-753 ± 6	-630 ± 7	-546 ± 6	-571 ± 10	-543 ± 9
Contribution of OC pools (%)‡						
Surface OC	nc¶	nc¶	56 ± 5	34 ± 8	25 ± 13	41 ± 11
Deep permafrost OC	nc¶	nc¶	44 ± 5	66 ± 8	75 ± 13	59 ± 11

- * Abundance-weighted average values with errors propagated, original values in Fig. S1;
- † Original values of long-chain *n*-alkanes and *n*-alkanoic acids from ref. (7);
- ‡ Estimated from the ^{14}C binary mixing model (Eq. 1), where the $\Delta^{14}\text{C}$ value of terrestrial biospheric OC is represented by that of hydroxyl phenols (derived from both surface OC and deep permafrost) while surface and deep permafrost end member values ($\Delta^{14}\text{C}_\text{S}$ and $\Delta^{14}\text{C}_\text{P}$) equal those of lignin phenols and plant wax lipids in each basin, respectively. Hence, $f_{\text{surface}} = (\Delta^{14}\text{C}_{\text{hydroxy phenols}} - \Delta^{14}\text{C}_{\text{plant wax lipids}}) / (\Delta^{14}\text{C}_{\text{lignin phenols}} - \Delta^{14}\text{C}_{\text{plant wax lipids}})$.
- § Based on the linear relationship between lignin phenol $\Delta^{14}\text{C}$ values and runoff ($\Delta^{14}\text{C} = 1.6018 \times \text{runoff} - 655$; Fig. 3a) and the runoff increasing rate of approximately 0.60 (Indigirka) to 0.74 mm/yr per year (the other GRARs) from 1964-2000 in Eurasian Arctic rivers (15, 16), lignin phenol $\Delta^{14}\text{C}$ values are estimated to be lower by 19‰ (0.60 mm/yr per year \times 20 years \times 1.6018 ‰/(mm/yr) for Indigirka) to 24‰ (0.74 mm/yr per year \times 20 years \times 1.6018 ‰/(mm/yr) for the other big GRARs) in 1985 as compared with those measured in 2004 (not considering the dilution of bomb ^{14}C in the atmosphere). The $\Delta^{14}\text{C}$ values of plant wax lipid and hydroxy phenols are assumed to remain the same as in 2004.
- ¶ Past OC contribution in Kalix and Ob is not calculated (nc) because the estimated $\Delta^{14}\text{C}$ values of surface OC (lignin phenols) are lower than those of terrestrial biospheric OC (hydroxy phenols).

SI Figures

Figure S1: The $\Delta^{14}\text{C}$ values of (a) individual lignin phenols and (b) individual hydroxy phenols as compared with the abundance-weighted average of vanillyl and syringyl phenols. All values are corrected for procedural blanks with the standard errors of analytical measurement propagated. Note that there is no significant offset in the average $\Delta^{14}\text{C}$ values between vanillyl and syringyl phenols from the same estuarine sediment (*t* test; $P > 0.05$).

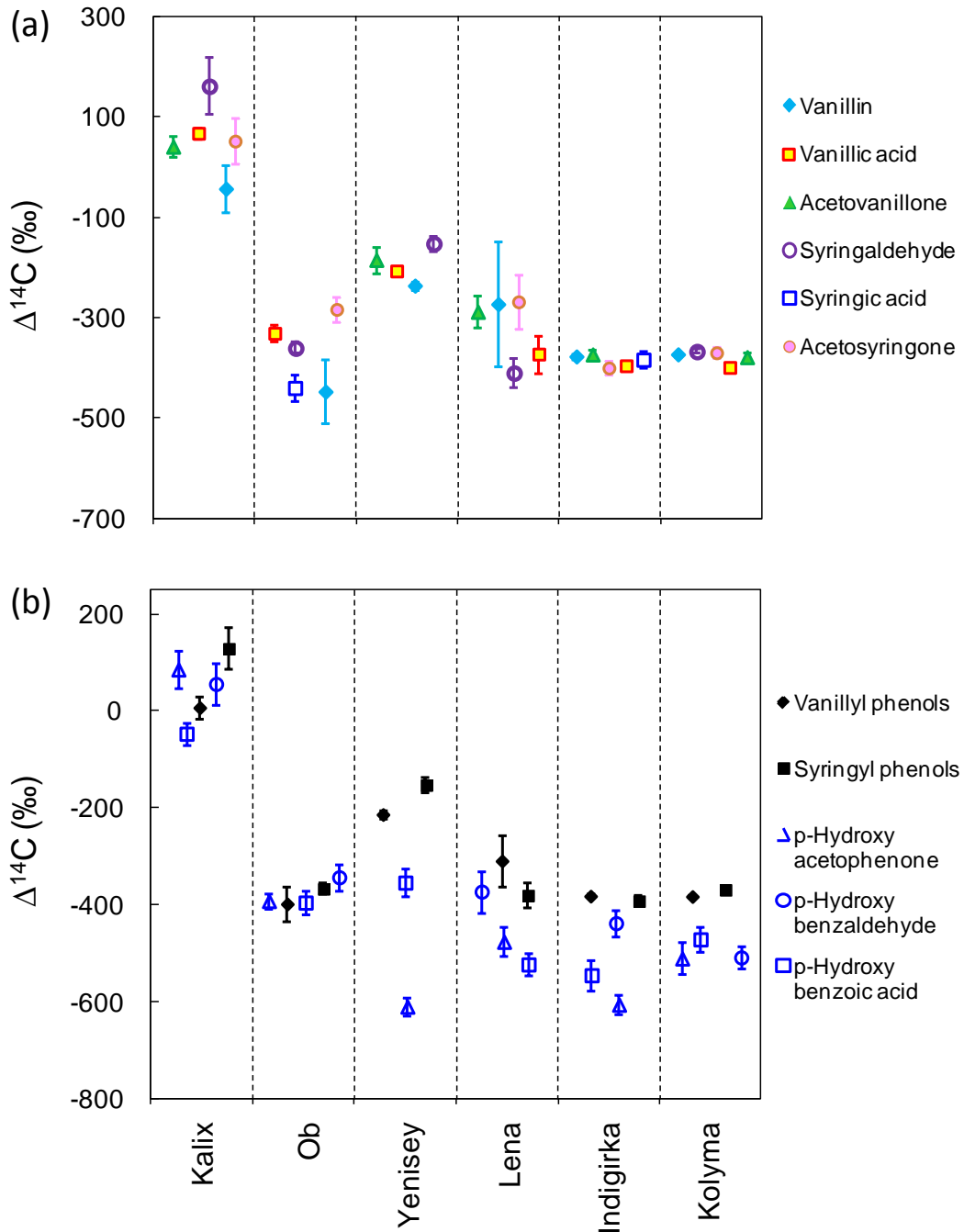


Figure S2: Correlation between drainage basin characteristics and the $\Delta^{14}\text{C}$ values of terrestrial markers. Error bars represent propagated standard error of analytical measurement. *Linear correlation is considered to be significant at a level of $P < 0.05$ and the R^2 values are used to compare the explanatory power of the variables. †Continuous permafrost coverage. Note that runoff, continuous permafrost and wetland coverage best explain the ^{14}C age of lignin phenols, plant wax lipids and hydroxy phenols across the Eurasian Arctic, respectively. ASCT: annual summer cumulative temperature (for months with a mean temperature above 0°C).

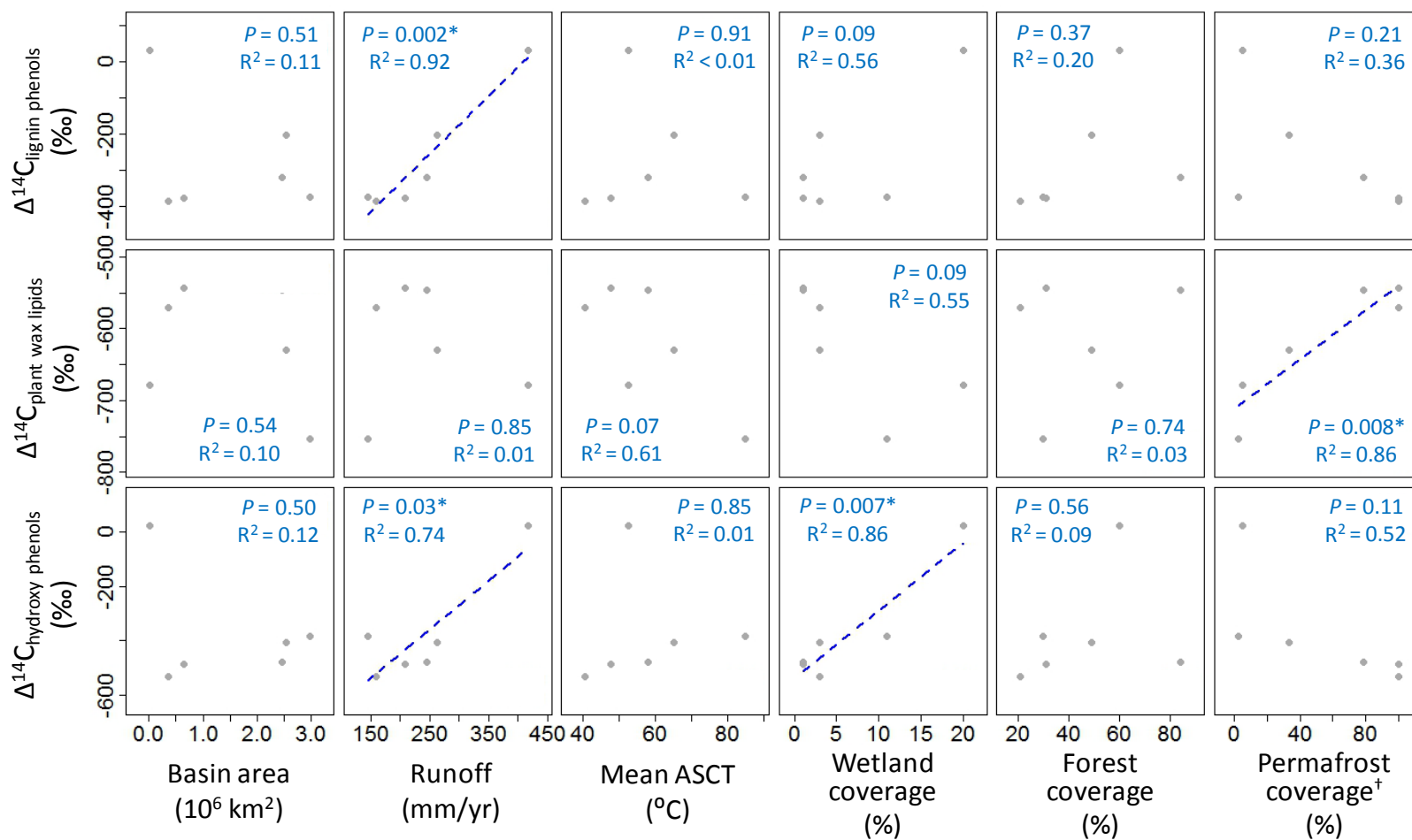
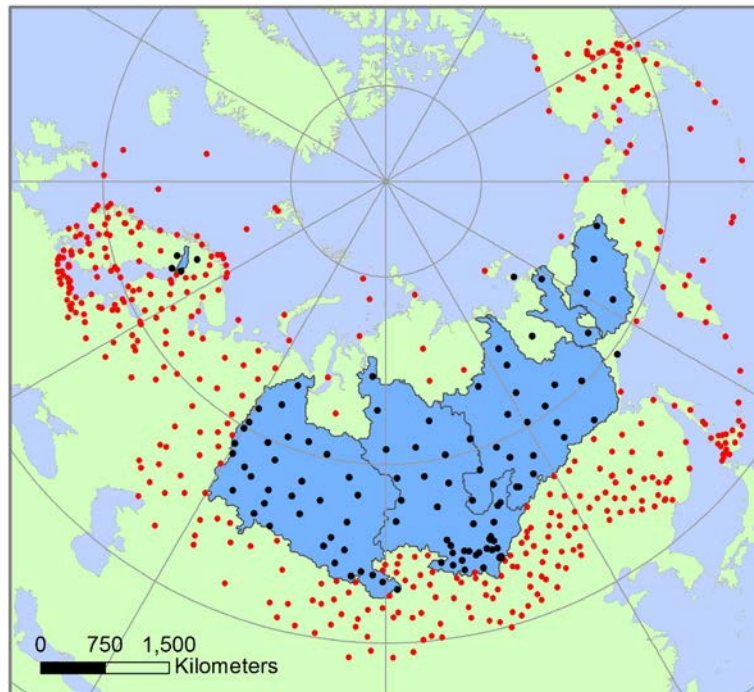


Figure S3: Map of climatic stations recorded in the GHCN-M database for each drainage basin. Blue area represents the watersheds of GRARs and Kalix River; black and red points refer to the location of climatic stations included in the calculation of regional temperature data and for the interpolation method, respectively.



References

1. Feng X, *et al.* (2013) ^{14}C and ^{13}C characteristics of higher plant biomarkers in Washington margin surface sediments. *Geochim. Cosmochim. Acta* 105:14-30.
2. Rinke A, *et al.* (2012) Arctic RCM simulations of temperature and precipitation derived indices relevant to future frozen ground conditions. *Global and Planetary Change* 80-81:136-148.
3. Hansen J, Sato M, & Ruedy R (2012) Perception of climate change. *Proceedings of the National Academy of Sciences* 109(37):14726-14727.
4. Frauenfeld OW, Zhang T, & McCreight JL (2007) Northern hemisphere freezing/thawing index variations over the twentieth century. *International Journal of Climatology* 27:47-63.
5. AMAP ed (1998) *AMAP Assessment Report: Arctic Pollution Issues, Arctic Monitoring and Assessment Programme* Oslo, Norway), p 859.
6. Ingri J, Widerlund A, & Land M (2005) Geochemistry of major elements in a pristine boreal river system; hydrological compartments and flow paths. *Aquatic Geochemistry* 11:57-88.
7. Gustafsson O, van Dongen BE, Vonk JE, Dudarev OV, & Semiletov IP (2011) Widespread release of old carbon across the Siberian Arctic echoed by its large rivers. *Biogeosciences* 8:1737-1743.
8. Holmes RM, *et al.* (2013) Climate change impacts on the hydrology and biogeochemistry of Arctic rivers. *Climatic Change and Global Warming of Inland Waters: Impacts and Mitigation for Ecosystems and Societies*, eds Goldman CR, Kumagai M, & Robarts RD (John Wiley & Sons, Ltd), pp 3-26.
9. Gordeev VV, Martin JM, Sidorov IS, & Sidorova MV (1996) A reassessment of the Eurasian river input of water, sediment, major elements, and nutrients to the Arctic Ocean. *American Journal of Science* 296:664-691.
10. Holmes RM, *et al.* (2002) A circumpolar perspective on fluvial sediment flux to the Arctic Ocean. *Global Biogeochemical Cycles* 16:GB1098, doi:10.1029/2001GB001849.
11. Rachold V, *et al.* (2004) Modern terrigenous organic carbon input to the Arctic Ocean. *The organic carbon cycle in the Arctic Ocean*, eds Stein R & Macdonald RW (Springer, Berlin, Heidelberg, New York), pp 33-56.
12. Stein R & Macdonald RW (2004) *The Organic Carbon Cycle in the Arctic Ocean* (Springer, Berlin).
13. van Dongen BE, Semiletov I, Weijers JWH, & Gustafsson O (2008) Contrasting lipid biomarker composition of terrestrial organic matter exported from across the Eurasian Arctic by the five great Russian Arctic rivers. *Global Biogeochemical Cycles* 22:GB1011, doi:10.1029/2007GB002974.
14. Vonk JE, van Dongen BE, & Gustafsson O (2008) Lipid biomarker investigation of the origin and diagenetic state of sub-arctic terrestrial organic matter presently exported into the northern Bothnian Bay. *Mar. Chem.* 112:1-10.
15. McClelland JW, Dery SJ, Peterson BJ, Holmes RM, & Wood EF (2006) A pan-arctic evaluation of changes in river discharge during the latter half of the 20th century. *Geophysical Research Letters* 33, L06715:doi: 10.1029/2006GL025753.
16. Peterson BJ, *et al.* (2002) Increasing river discharge to the Arctic Ocean. *Science* 298:2171-2173.